The Value of Second-look Ultrasound and Mammography for Assessment and Biopsy of MRI-detected Breast Lesions

Stephanie Tina Sauer, MD, Julius Geerling, Sara Aniki Christner, MD, Tanja Schlaiß, MD, Matthias Kiesel, MD, Anne Cathrine Scherer-Quenzer, MD, Lukas Müller, MD, Julius Frederik Heidenreich, MD, Thorsten Alexander Bley, MD, Jan-Peter Grunz, MD

Rationale and Objectives: Suspicious lesions detected in multiparametric breast MRI can be further analyzed with second-look ultrasound (SLUS) and/or mammography. This study aims to assess the value of second-look imaging in selecting the appropriate biopsy method for different lesion characteristics.

Materials and Methods: Between January 2021 and December 2023, 212 women underwent contrast-enhanced multiparametric breast MRI at 3 Tesla. A total of 241 suspicious lesions (108 malignancies, 44.8%) were further assessed with SLUS and second-look mammography. Subsequent image-guided biopsy of each lesion was performed using the most suitable modality. Size-dependent lesion detection rates in SLUS and mammography were compared by means of the McNemar test.

Results: Lesions referred to MRI-guided biopsy were predominantly ≤ 10 mm in size (52.8%). SLUS allowed for higher detection rates than mammography in mass lesions (55.6% [95% confidence interval 46.4–64.4%] versus 16.7% [10.6–24.3%]; $p < 0.001$) with a particularly high sensitivity for malignant mass lesions > 10 mm (88.5% [69.9–97.6%]). In contrast, the detection rate for malignant non-mass lesions was lower in SLUS than in second-look mammography (22.0% [11.5–36.0%] versus 38.0% [24.7–52.8%]; $p < 0.001$). The malignancy rates in ultrasound-, mammography-, and MRI-guided biopsies were 53.7%, 55.2%, and 35.0%, respectively.

Conclusion: SLUS is an excellent tool for further assessment and biopsy of suspicious mass lesions > 10 mm without associated calcifications. In contrast, supplemental ultrasound is of limited value in the evaluation and biopsy guidance of suspicious non-mass lesions compared to second-look mammography.

Key Words: Breast imaging; MRI-only lesions; Biopsy; Second-look ultrasound; Assessment.

Abbreviations: BIRADS breast imaging reporting and data system, **SLUS** second-look ultrasound

INTRODUCTION

Contrast-enhanced MRI of the breast is known to improve breast cancer detection with a high sensitivity in diagnostic settings and for screening purposes. The number of examinations has therefore increased significantly in the last decade (1–5). Breast MRI is a functional imaging technique relying on the increased permeability of vessels for gadolinium due to tumorous neoangiogenesis. Therefore, the procedure has a different pathophysiological background than ultrasound or mammography and allows for additional detection of lesions in up to 32% of exams, albeit at the cost of a relatively high false positive rate (6–9).

If breast lesions present with suspicious imaging features, histopathological evaluation is necessary. To achieve that,

Acad Radiol 2025; 32:1818–1826

From the Department of Diagnostic and Interventional Radiology, University Hospital Würzburg, Oberdürrbacher Straße 6, 97080 Würzburg, Germany (S.T.S., J.G., S.A.C., J.F.H., T.A.B., J-P.G.); Department of Obstetrics and Gynecology, University Hospital Würzburg, Josef-Schneider-Str. 4, 97080 Würzburg, Germany (T.S., M.K., A.C.S-Q.); Department of Diagnostic and Interventional Radiology, University Hospital Mainz, Langenbeckstr. 1, 55131 Mainz, Germany (L.M.); Department of Radiology, University of Wisconsin–Madison, 600 Highland Ave, 53792 Madison, WI (L.M., J.F.H., J-P.G.). Received August 11, 2024; revised October 20, 2024; accepted October 22, 2024. **Address correspondence to**: J-P.G. e-mail: Grunz_J@ukw.de

https://doi.org/10.1016/j.acra.2024.10.037

vacuum-assisted biopsy-systems have been developed for the use in MRI suites, however, their implementation into clinical routine is expensive and time consuming (10). Second-look ultrasound (SLUS), a targeted sonography examination following the MRI scan, allows for image-guided biopsy with easier, cheaper, and faster assessment. However, detection rates in SLUS range from 22.6 to 82.1% depending on the lesion type, size, and experience of the investigator (11). Various studies confirm the necessity of MRI-guided biopsy for SLUS-occult lesions due to a considerable percentage of malignant lesions among them (up to 53.8%) (5,12–14). Significantly less data is available for the use of second-look mammography and tomosynthesis after breast MRI (13,15–17). While Clauser et al. reported an imaging correlate for MRI findings in up to 75% of cases when combining SLUS and second-look tomosynthesis (13), this study was focused on preoperative breast MRI and transferability of results to other imaging tasks, such as screening in high-risk women or diagnostic workup, may be limited.

In order to address this research gap in the current literature, we provide an in-depth analysis of morphological findings, selected biopsy methods, and histopathological correlates for suspicious lesions detected in breast MRI. Thereby, we aim to derive a practical approach for the use of SLUS and supportive mammography in secondary lesion assessment and biopsy.

MATERIAL AND METHODS

Study Sample

This retrospective study was conducted at a tertiary-care university hospital and approved by the local ethics committee (IRB number 20240117 04). The need for additional written informed consent was waived. Between January 2021 and December 2023, a total of 271 women underwent contrast-enhanced breast MRI with subsequent indication for histopathological assessment of a suspicious lesion. Indications for MRI included staging purposes in case of biopsy-proven malignancy, follow-up imaging after breast cancer therapy, further assessment of abnormal findings in previous mammography or ultrasound examinations, breast-related symptoms, or screening in high-risk patients according to the guidelines of the German Consortium for Hereditary Breast and Ovarian Cancer (1). A histopathological reference standard was deemed mandatory for study inclusion, adhering to the Standards for Reporting of Diagnostic Accuracy (STARD) (18). Only patients with an image-guided biopsy of an intramammary lesion were included. Exclusion criteria comprised breast surgery for histopathological assessment, patients not undergoing in-house follow-up, and suspected diagnosis of breast implant associated anaplastic large cell lymphoma with only peri-implant fluid or suspicious lymph nodes. Applying these criteria, a total of 212 women were included in the final study sample. Patient inclusions and exclusions are shown in Figure 1. Diagnostic MRI reports were analyzed for lesion characterization descriptors and study-specific parameters (e.g., MRI indication, menopausal status). Additional information and histopathological results were derived from the clinical information system (SAP, Walldorf, Germany).

Diagnostic Breast MRI

Diagnostic breast MRI was performed on one of two 3 Tesla systems (Magnetom Skyra [January 2021 until April 2022] or Vida fit [May 2022 until December 2023], both Siemens Healthineers, Erlangen, Germany). Patients were scanned in prone position with a dedicated 16-channel Sentinelle breast coil (Siemens Healthineers). According to national recommendations, examinations were conducted in the second week of the menstrual cycle whenever possible (19). The multiparametric scan protocol encompassed the following: A transversal T2-weighted turbo spin-echo sequence with fat suppression (TR 10220 ms / TE 81 ms, 3 mm slice thickness, in-plane resolution of 0.98 × 0.98 mm, field of view of 380 × 380 mm^2, and acquisition matrix of 384 × 384 pixels, Dixon fat suppression), a transversal T1-weighted gradient-echo sequence

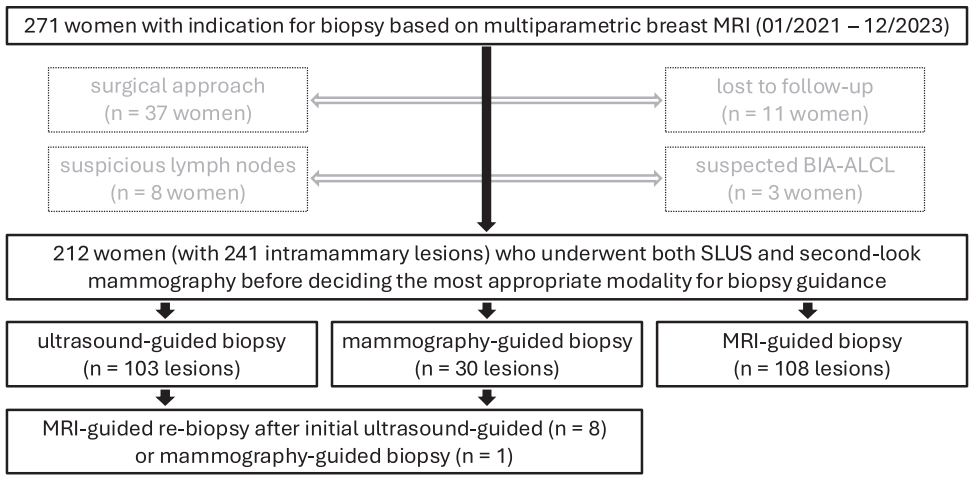

Figure 1. Study Sample Overview.

with and without fat suppression, contrast-enhanced T1-weighted sequences with fat suppression and post-contrast subtracted images (TR 5.47 ms/ TE 2.46 ms, 1.5 mm slice thickness, in-plane resolution of 0.9 × 0.9 mm, field of view of 380 × 380 mm^2, acquisition matrix 349 × 416 pixels, Dixon fat suppression) and diffusion-weighted images based on single-shot echo-planar imaging with spectral-attenuated inversion recovery for fat suppression and computed apparent diffusion coefficient maps. For intravenous contrast, a gadolinium-based contrast agent was administered with a dosage of 0.1 mmol/kg body weight (Gadovist, Bayer Vital GmbH, Leverkusen, Germany). If the indication for a biopsy was determined based on an exam from outside of our institution, the underlying MRI protocol also had to adhere to the national recommendations; otherwise, a re-examination with the standardized in-house protocol was scheduled.

Assessment

Every patient with an indication for biopsy based on MRI underwent additional imaging with SLUS using a high-resolution ultrasound system with a linear transducer of 10 – 18 MHz (Acuson 2000 or Sequoia, Siemens Healthineers). Additional full-field digital mammography or tomosynthesis with synthetic mammography was conducted with state-of-the-art scanner hardware (3Dimensions or Dimensions, Hologic, Marlborough, Massachusetts, USA) in all cases where no mammography had been performed within the last 3 months. This approach guarantees that each lesion was examined with all three imaging techniques (i.e., MRI, SLUS, and second-look-mammography) before deciding on the most suitable modality for biopsy guidance. Case reading and SLUS was performed by one of two board-certified radiologists with 7 – 9 years of experience in the field. The same radiologist was responsible for all imaging studies in one patient, i.e., reading the MRI and mammograms, performing SLUS, and checking the concordance of image findings and histopathological results. Whenever a suspicious lesion displayed a correlate in ultrasound, this biopsy method was preferred over mammography- and MRI-guided biopsy due to lower complication rates and costs, time saving, as well as higher patient comfort (5). Figure 2 demonstrates a case of a BIRADS 5 lesion visible in all modalities. In lesions with no correlate in SLUS but

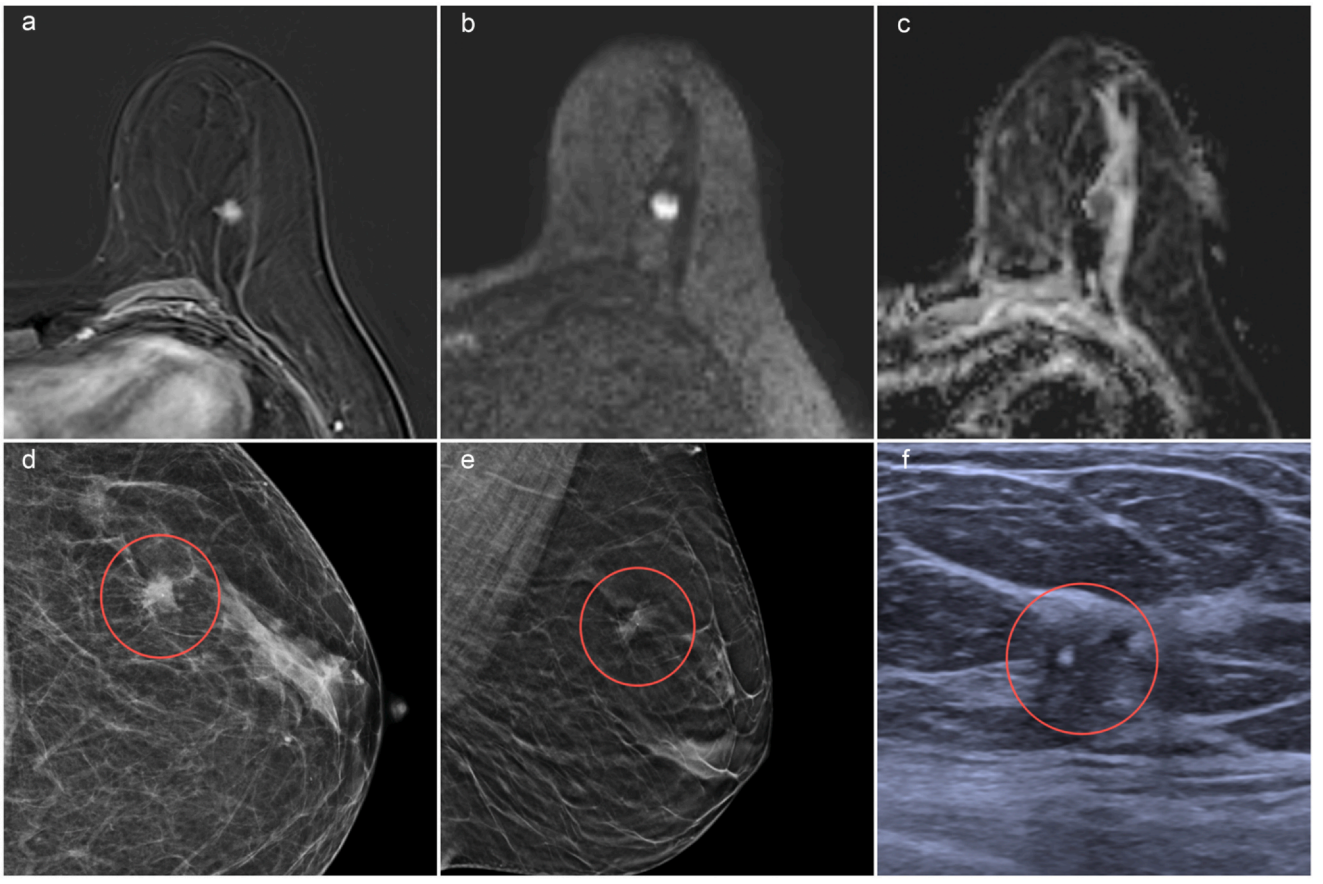

Figure 2. Enhancing mass lesion of 12 mm (**a**, early subtraction T1 post-contrast) in the upper outer quadrant of the left breast in a 56-year-old woman. Multiparametric breast MRI was performed as follow-up of breast cancer on the contralateral side. High b-value diffusion-weighted imaging (**b**, b = 1600 s/mm^2) and corresponding apparent diffusion coefficient-map (**c**) show suspicious diffusion restriction (BIRADS 5). Craniocaudal (**d**) and mediolateral oblique projection of digital mammography (**e**, 6 mm thick slab tomosynthesis) and second-look ultrasound also depict the mass lesion. Ultrasound-guided biopsy was performed with the histopathological diagnosis being an invasive breast cancer of no special type (G2).

in mammography, especially in lesions associated with (micro-) calcifications, mammography-guided biopsy was preferred over MRI-guided biopsy. Only lesions without a correlate in both SLUS and mammography were referred to MRI-guided biopsy. Additionally, if histopathological correlation revealed incongruent results after ultrasound or mammography-guided biopsy, patients were referred to MRI-guided re-biopsy.

Ultrasound-guided Biopsy

Whenever a lesion was visible in SLUS, ultrasound-guided core-needle biopsy using a 12 or 14 G needle (Histocore, BIP, Türkenfeld, Germany) in coaxial technique was performed. Patients were brought either in supine or decubitus position for the intervention. Intralesional needle position was confirmed and documented in two orthogonal planes. If concordance with previous MRI could not be established or the lesion was no longer visible after biopsy, a marker (UltraClip Dual Trigger Breast Tissue Marker, BD, Franklin Lakes, New Jersey, USA) was placed at the biopsy site to allow for eventual re-MRI comparison. Figure 3 shows a 59-year-old woman undergoing ultrasound-guided biopsy with placement of a biopsy site marker and subsequent MRI-guided re-biopsy due to incongruent results.

Mammography-guided Biopsy

For lesions with a mammographic correlate, a mammography-guided biopsy was performed on an upright system (Hologic 3Dimensions, Hologic) using 9 G-needles with a vacuum-assisted biopsy system (Brevera, Hologic). Depending on the biopsy site, patients adopted either an upright or decubitus position using a dedicated chair (Mammography Positioning Chair, Akrus, Elmshorn, Germany). Scout-images for determining the biopsy localization were performed by means of tomosynthesis and stereotactic images were obtained to control the needle position. After the procedure, a biopsy site marker (SecurMark, Hologic) was inserted to allow for comparison with eventual re-MRI in case of incongruent histopathological results. Samples were x-rayed to confirm representative biopsy in case of calcification-containing lesions.

MRI-guided Biopsy

For MRI-guided biopsy, a shortened scan protocol was applied, which included the same transversal T1-weighted gradient-echo sequence with and without fat suppression and the contrast-enhanced T1-weighted sequences with fat suppression and post-contrast subtraction (two sequences after contrast admission) as mentioned above. An 8-channel breast biopsy coil was used for all procedures (Noras MRI products, Höchberg, Germany). For immobilization of the breast and guiding the biopsy, a post-and pillar system (Noras MRI products) with a 10 G needle for vacuum-assisted biopsy (Encore Enspire, BD) was employed. Standard T1-weighted post-contrast imaging was used to verify the correct needle position before and after biopsy. A radiopaque marker (SenoMark UltraCor MRI Breast Tissue Marker, BD) was inserted to allow for correlation with subsequent mammography.

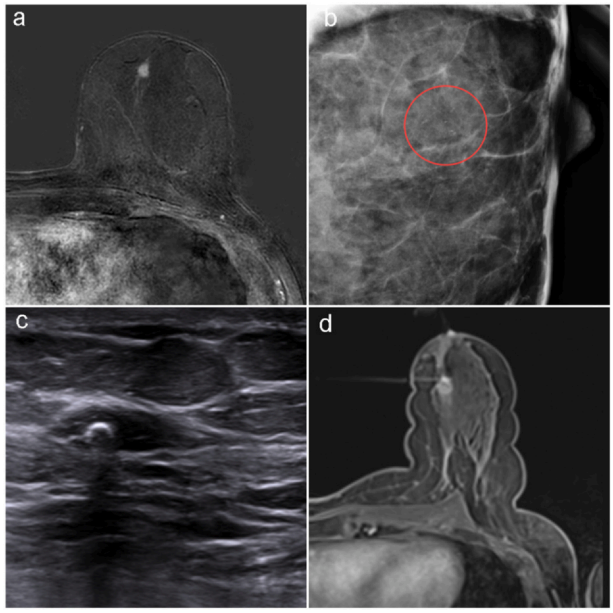

Figure 3. A 59-year-old woman underwent multiparametric breast MRI (**a**, early subtraction T1 post-contrast) due to left-sided pathologic nipple discharge with a suspicious lesion of 10 mm in the inner lower quadrant (BIRADS 4). Additional magnification view (**b**) showed a group of amorphous calcifications (circle) in the retromamillar area. In second-look ultrasound, an oval, hypoechoic circumscribed mass was detected in the lower inner quadrant. Ultrasound-guided biopsy (**c**, with biopsy site marker in situ) resulted in the diagnosis of a benign fibroadenoma (B2 lesion), which was considered incongruous with the suspicious finding in MRI. Subsequent MRI-guided biopsy (**d**, compressed breast with inserted coaxial canula) revealed an invasive breast cancer of no special type (G2) with associated ductal carcinoma in situ.

Statistics

For data analyses, dedicated statistical software was employed (SPSS Statistics 29.0.1, IBM, Armonk, New York, USA). Following Kolmogorov-Smirnov tests for assessment of normal distribution in continuous variables, normally distributed items are reported as mean ± standard deviation. Ordinal and nominal-scaled data are presented as absolute and relative frequencies with calculation of median values and interquartile ranges. For correlation of lesion size and malignancy, the Spearman-Rho coefficient was calculated. In case of mammography-guided biopsy, a cross table was used to evaluate the association with suspicious microcalcifications. The same method was applied for correlation of biopsy modality and histopathological malignancy as well as for the association between maximum axial lesion size and MRI-guided biopsy. Lesion detectability was calculated for each modality as the number of correctly identified lesions divided by the sum of true positives and false negatives. To compare lesion detectability between SLUS and

mammography, McNemar tests were performed (individually for mass and non-mass lesions as well as for lesions ≤ 10 mm and > 10 mm in size). P values < 0.05 were considered to represent statistical significance.

RESULTS

Sample Characteristics

A total of 212 women were included in the analysis with a mean age of 52.9 ± 13.6 years, of whom 84 (39.6%) were premenopausal, 87 (41.0%) postmenopausal, and 23 (10.8%) under endocrine treatment. Patients underwent MRI mainly due to staging purposes (31.5%) or high-risk screening (29.5%).

Overall, 241 suspicious lesions were evaluated with 121 (50.2%) in the left breast and 120 (49.8%) in the right breast, predominantly in the upper outer quadrant (34.0%). Nine lesions (3.7%) were classified as focus, while 126 (52.3%) mass lesions and 106 (44.0%) non-mass lesions were reported. Mean overall lesion size was 17.2 ± 17.4 mm, with 125 lesions (51.9%) being larger than 10 mm. Most lesions (97.1%) were classified as BIRADS 4 and 5, the remaining BIRADS 0 (1.7%) and BIRADS 3 (1.2%) lesions were referred to biopsy after interdisciplinary board discussion. Mass lesions were mainly characterized as oval shaped (41.2%), with irregular margins (42.1%) and homogenous internal enhancement pattern (43.7%), whereas non-mass lesions predominantly displayed a linear distribution (34.9%) with heterogeneous internal pattern (40.6%). Due to the small sample size, foci were subsumed under focal non-mass lesions for statistical evaluation.

Histopathological diagnosis revealed 108 malignant (44.8%) and 133 benign lesions (55.2%) with four B4 lesions and one B3 lesion (a multifocal flat epithelial atypia) being recategorized as malignant after surgery. The most common histopathological subtypes were carcinoma of no special type (43.5%) and ductal / lobular carcinoma in situ (38%). Statistical analysis revealed a weak positive correlation between malignancy and lesion size with a Spearman-Rho coefficient of 0.13 ($p < 0.05$). In patients who underwent breast MRI for preoperative staging purposes (n = 76), 38 suspicious additional lesions were found each in the ipsilateral and the contralateral breast. Malignancy rates among these were 52.6% (20 malignant lesions) in the ipsilateral breast and 42.1% (16 malignant lesions) in the contralateral breast. In high-risk screening patients, the malignancy rate of MRI-detected lesions was 39.4%. Meanwhile, malignancy rates for follow-up imaging after breast cancer therapy and for further assessment including breast-related symptoms were 46.1% and 43.6%, respectively. Detailed lesion and patient data are provided in Table 1.

Lesion Detectability

Overall, the detectability of lesions was higher in SLUS (39.8% [95% confidence interval 33.6–46.3%]) than in second-look mammography (20.3% [15.4–26%]; $p < 0.001$). In the ensuing subgroup analyses, the superiority of SLUS over mammograms was size-independently confirmed for mass lesions (55.6% [46.4–64.4%] versus 16.7% [10.6–24.3%]; $p < 0.001$). For non-mass lesions, however, no significant difference was ascertained between the two modalities (22.6% [15.3–31.4%] versus 24.3% [16.8–33.2%]; $p = 0.878$). In SLUS, mass lesions larger than 10 mm were more often detected (79.1% [64.0–90.0%]) than smaller masses (43.4% [32.5–54.7%]). The same tendency was observed for mammography (25.6% [13.5–41.2%] versus 12.0% [5.9–21.0%]) (Table 2). Regardless of size and morphology, lesions associated with suspicious microcalcifications were more often detected with second-look mammography than SLUS (Supplemental Table S1).

Analyzing the subgroup of malignant lesions, SLUS again allowed for a better detection rate than mammography (48.1% [38.4–58.0%] versus 31.5% [22.9–41.1%]; $p < 0.001$). SLUS displayed a particularly high sensitivity for malignant mass lesions (55.6% of all mass lesions versus 70.7% of malignant mass lesions). In contrast, the detection rate of non-mass lesions in SLUS was largely independent of their characterization (22.6% of all lesions versus 22.0% of malignant lesions). Notably, in mammography, the detection rate for non-mass malignancies was better than for non-mass lesions in general (24.3% of all lesions versus 38.0% of malignant lesions). Detailed results are presented in Table 3.

Biopsy Methods

Ninety-five lesions (39.4%) were solely biopsied by means of SLUS. An additional eight lesions underwent initial ultrasound-guided biopsy with subsequent re-biopsy in MRI. In contrast, only one lesion with a mammographic, non-calcified correlate required MRI-guided re-biopsy. Mammography-guided biopsy with concordant results was performed in 29 lesions (12.0%). Overall, 23 of 30 mammography-guided biopsies contained calcifications (76.7%). MRI-guided biopsy was performed in 117 cases (i.e., 108 lesions without a correlate in SLUS and second-look mammograms in addition to the nine re-biopsies; 48.5%). The malignancy rates in ultrasound-, mammography-, and MRI-guided biopsy were 53.7%, 55.2%, and 35.0%, respectively. Lesions referred to MRI-guided biopsy were predominantly ≤ 10 mm (52.8%), whereas the majority of ultrasound- (58.9%) and mammography-guided biopsies (62.1%) targeted lesions > 10 mm.

DISCUSSION

In this study, we analyzed the relevance of second-look ultrasound and mammography in the assessment and biopsy of 241 suspicious lesions in contrast-enhanced breast MRI. As a major finding, we were able to show that ultrasound is especially helpful in the detection and biopsy of mass lesions greater than 10 mm, whereas the detection rates of non-mass

TABLE 1. Lesion and Patient Characteristics

Lesion type		Menopausal status		Mass shape	
Focus	9 (3.7%)	Premenopausal	84 (39.6%)	Round	27 (21.4%)
Mass	126 (52.3%)	Postmenopausal	87 (41.0%)	Oval	52 (41.2%)
Non-mass	106 (44.0%)	Endocrine treatment	23 (10.8%)	Irregular	47 (37.3%)
		Unknown	18 (8.5%)		
Lesion laterality		Imaging task		Mass margin	
Left	121 (50.2%)	Staging	76 (31.5%)	Circumscribed	42 (33.3%)
Right	120 (49.8%)	Follow-up	39 (16.2%)	Irregular	53 (42.1%)
		High-risk screening	71 (29.5%)	Spiculated	31 (24.6%)
		Other	55 (22.8%)		
Quadrant		Fibroglandular tissue		Mass internal pattern	
Upper outer	82 (34.0%)	a	16 (7.5%)	Homogenous	55 (43.7%)
Upper inner	52 (21.6%)	b	94 (44.3%)	Heterogenous	47 (37.3%)
Lower inner	36 (14.9%)	c	66 (31.1%)	Rim	24 (19.0%)
Lower outer	61 (23.3%)	d	36 (17.0%)		
Central	10 (4.1%)				
Lesion size		Background enhancement		Non-mass distribution	
≤ 10 mm	116 (48.1%)	a	65 (30.7%)	Focal	29 (27.4%)
> 10 mm	125 (51.9%)	b	93 (43.9%)	Linear	37 (34.9%)
		c	47 (22.2%)	Segmental	22 (20.8%)
		d	7 (3.3%)	Regional	15 (24.2%)
				Diffuse	3 (2.8%)
B-Category		BIRADS category		Non-mass pattern	
B1	2 (0.8%)	0	4 (1.7%)	Homogenous	35 (33.0%)
B2	104 (43.2%)	3	3 (1.2%)	Heterogenous	43 (40.6%)
B3	27 (11.2%)	4	194 (80.5%)	Clumped and clustered	28 (26.4%)
B4	5 (2.1%)	5	40 (1.6%)		
B5a	39 (16.2%)				
B5b	64 (26.6%)				
Lesion characterization		Cancer subtype		Concomitant malignancy	
Malignant	108 (44.8%)	No special type	47 (43.5%)	Ipsilateral	20 (52.6%)
Benign	133 (55.2%)	Invasive-lobular	15 (13.9%)	Contralateral	16 (42.1%)
		In-situ carcinoma	41 (38.0%)		
		Other	5 (4.6%)		

lesions were comparable between second-look mammography and ultrasound (with the former facilitating better delineation of lesions associated with suspicious calcifications). Due to a lack of visibility in conventional diagnostics, lesions smaller than 10 mm were predominantly referred to MRI-guided biopsy in the present sample, which resulted in a lower malignancy rate compared to ultrasound- or mammography-guided biopsy. Our study underlines the need for a nuanced approach to assess MRI-detected lesions with second-look diagnostics in a broad spectrum of indications.

The investigated patient group represents a clinical routine population at a tertiary-care university hospital, including the most common imaging tasks for multiparametric breast MRI, such as staging, screening, and breast-related symptoms. It must be noted, however, that the screening exams at our hospital are exclusively performed in high-risk patients, contributing to the relatively high percentage of biopsy-proven malignancies. The distribution of fibroglandular tissue (mainly type b and c) and the location of lesions (predominantly in the upper outer quadrant) can also be considered representative of clinical routine. The rate of malignancies among additional lesions detected in MRI for staging purposes (53.6% for the ipsilateral and 42.1% for the contralateral breast) is also in line with literature (20). While the overall malignancy rate of 44.8% was certainly influenced by the variable clinical settings, the high amount (48.1%) of lesions ≤ 10 mm may reflect the superior sensitivity of MRI compared to conventional diagnostic procedures. The main strength of this study is the standardized approach to inclusion and assessment, assuring that every MRI-detected lesion underwent image-guided biopsy.

Due to the increasing use of multiparametric breast MRI, the development of a purposeful algorithm for assessment of MRI-

TABLE 2. Overall Lesion Detectability in Second-look Ultrasound and Mammography

Detectability	Second-look Ultrasound	Second-look Mammography	P Values
Mass lesions	70/126	21/126	< 0.001
	55.6% (46.4 – 64.4%)	16.7% (10.6 – 24.3%)	
> 10 mm	34/43	11/43	< 0.001
	79.1% (64.0 – 90.0%)	25.6% (13.5 – 41.2%)	
≤ 10 mm	36/83	10/83	< 0.001
	43.4% (32.5 – 54.7%)	12.0% (5.9 – 21.0%)	
Non-mass lesions	26/115	28/115	0.878
	22.6% (15.3 – 31.4%)	24.3% (16.8 – 33.2%)	
> 10 mm	19/83	21/83	0.856
	22.9% (14.4 – 33.4%)	25.3% (16.4 – 36.0%)	
≤ 10 mm	7/32	7/32	> 0.999
	21.9% (9.3 – 40.0%)	21.9% (9.3 – 40.0%)	
Overall	96/241	49/241	< 0.001
	39.8% (33.6 – 46.3%)	20.3% (15.4 – 26.0%)	

Note. – Lesion detectability is reported in form of absolute and relative frequencies with 95% confidence intervals in parentheses.

TABLE 3. Detectability of Malignant Lesions in Second-look Ultrasound and Mammography

Detectability	Second-look Ultrasound	Second-look Mammography	P Values
Mass lesions	41/58	15/58	< 0.001
	70.7% (57.3 – 81.9%)	25.9% (15.3 – 39 –0%)	
> 10 mm	23/26	9/26	< 0.001
	88.5% (69.9 – 97.6%)	34.6% (17.2 – 55.7%)	
≤ 10 mm	18/32	6/32	0.012
	56.3% (37.7 – 73.6%)	18.8% (7.2 – 36.4%)	
Non-mass lesions	11/50	19/50	0.096
	22.0% (11.5 – 36.0%)	38.0% (24.7 – 52.8%)	
> 10 mm	8/36	14/36	0.146
	22.2% (10.1 – 39.2%)	38.9% (23.1 – 56.5%)	
≤ 10 mm	3/14	5/14	0.687
	21.4% (4.7 – 50.8%)	35.7% (12.8 – 64.9%)	
Overall	52/108	34/108	0.020
	48.1% (38.4 – 58.0%)	31.5% (22.9 – 41.1%)	

Note. – Lesion detectability is reported in form of absolute and relative frequencies with 95% confidence intervals in parentheses.

detected lesions is essential to reduce overdiagnosis and to refer patients to the most suitable biopsy modality. SLUS is a thoroughly investigated and broadly available technique, however, its quality is highly dependent on the examiner's level of expertize not only in breast ultrasound but also in reading MRI exams. Furthermore, SLUS can be time consuming, especially if the lesions in question are small. In our study, the number of lesions ≤ 10 mm was nearly 50% with an overall detection rate in SLUS of 39.8% (48.1% in malignancies). Considering a detection rate of 79.1% in mass lesions > 10 mm (88.5% in malignancies), lesion size and morphology appear to be of utmost importance for SLUS. This finding is in line with the majority of recent studies, as well as with the meta-analysis by Spick et al. (11,13,21–23). One major drawback of previous studies lies in the fact that they do not disclose whether the same reader conducted MRI reading and SLUS. In our research, SLUS was always performed by the examiner who previously read the MRI, reviewed the mammography, and finally checked the concordance of image findings and histopathological results. This holistic approach reduces the risk of non-consideration of previous findings in a multimodal imaging scenario. Taking into account its high sensitivity compared with mammography even in smaller lesions, SLUS appears appropriate for mass lesions of all sizes. However, our data should not be considered suggestive of omitting second-look mammograms for mass lesions in general, since the examiner performing SLUS could have been influenced by the mammography results. Furthermore, mammograms were particularly helpful in identifying lesions associated with suspicious calcifications.

Non-mass lesions appear to pose an entirely different challenge to breast radiologists with no significant differences observed between the absolute detection rates in SLUS and mammography. When analyzing only malignant non-mass lesions, the detection rate of mammography was substantially higher at 38.0%, while no changes were found for SLUS. This finding may be attributed to mammograms facilitating

superior delineation of suspicious calcifications, which are considered indicative of ductal carcinoma in situ. Our results are in line with the aforementioned study by Clauser et al., who reported that adding digital breast tomosynthesis to SLUS improves detection rates in particular for non-mass lesions (13). In a similar approach, Mariscotti et al. used additional tomosynthesis after negative SLUS to identify 64% of the MRI-detected, SLUS-occult lesions (16).

In a recent investigation comparing the costs for image-guided breast biopsies in the U.S. from July 2020 to April 2021, Ali et al. were able to show that MRI-guided biopsies are substantially more expensive than using conventional imaging (costs of MRI-guided, stereotactic, and ultrasound-guided biopsy: $1611, $826, and $356) (24). Using SLUS for image-guidance, 7.8% of biopsies in the present study (8 of 103) missed the intended target lesion derived from MRI, subsequently leading to MRI-guided re-biopsy. While we only biopsy findings based on second-look imaging if we are confident of having identified the correct target lesion, the intervention itself is still dependent on examiner experience, patient preferences and scanner capacities, among others. Taking into account that a substantial percentage of malignant lesions remains without a clear correlate in second-look imaging (5,12–14) and compared to the high rates of false benign findings reported in the literature, e.g., by Chikarmane et al. (25), our re-biopsy rate after SLUS appears to be reasonable. This may in part be attributed to our low threshold to perform MRI-guided biopsy in ambiguous cases.

Several methodological limitations must be acknowledged: First, the study followed a monocentric retrospective design, which limits the generalizability over different diagnostic centers. Second, the effect of tomosynthesis was not separately evaluated since tomosynthesis is not a regular addition to mammography in the second-look assessment of suspicious MRI lesions at our institution based on clinical standards. However, both full-field digital mammography (n = 136) and synthetic mammograms computed from tomosynthesis (n = 76) were included in the investigated sample of second-look mammograms. Third, we did not evaluate which morphological descriptors correlated with detectability of lesions in SLUS or mammography. This aspect should be assessed in future studies, especially taking into account the efforts of "downgrading" MRI-detected lesions by associating them with typically benign features in SLUS or mammograms (22,23).

CONCLUSION

Comparing morphological findings, biopsy modalities, and histopathological results for 241 lesions classified as suspicious in multiparametric breast MRI, our data suggest that second-look ultrasound is an excellent tool for further assessment of mass lesions without calcifications, especially if their diameter is greater than 10 mm. In contrast, supplemental ultrasound appears to be of limited value in the evaluation and biopsy guidance of non-mass lesions if second-look mammography is available.

DECLARATION OF COMPETING INTEREST

The authors declare the following financial interests/personal relationships which may be considered as potential competing interests: Jan-Peter Grunz [grant number Z-3BC/02] is financially supported by the Interdisciplinary Center of Clinical Research Würzburg. Stephanie Sauer, Thorsten Bley, and Jan-Peter Grunz report a relationship with Siemens Healthineers that includes consulting or advisory and paid expert testimony. The Department of Diagnostic and Interventional Radiology receives ongoing research funding by Siemens Healthineers outside of the presented work.

APPENDIX A. SUPPORTING INFORMATION

Supplemental data associated with this article can be found in the online version at doi:10.1016/j.acra.2024.10.037.

REFERENCES

1. Bick U, Engel C, Krug B, et al. High-risk breast cancer surveillance with MRI: 10-year experience from the German consortium for hereditary breast and ovarian cancer. Breast Cancer Res Treat 2019; 175:217–228.
2. Kuhl C, Weigel S, Schrading S, et al. Prospective multicenter cohort study to refine management recommendations for women at elevated familial risk of breast cancer: the EVA trial. J Clin Oncol 2010; 28:1450–1457.
3. Eisen A, Fletcher GG, Fienberg S, et al. Breast magnetic resonance imaging for preoperative evaluation of breast cancer: a systematic review and meta-analysis. Can Assoc Radiol J 2024; 75.
4. Bakker MF, de Lange SV, Pijnappel RM, et al. Supplemental MRI screening for women with extremely dense breast tissue. N Engl J Med 2019; 381:2091–2102.
5. Mann RM, Balleyguier C, Baltzer PA, et al. Breast MRI: EUSOBI recommendations for women's information. Eur Radiol 2015; 25:3669–3678.
6. Mann RM, Cho N, Moy L. Breast MRI: state of the art. Radiology 2019; 292:520–536.
7. Mann RM, Hoogeveen YL, Blickman JG, et al. MRI compared to conventional diagnostic work-up in the detection and evaluation of invasive lobular carcinoma of the breast: a review of existing literature. Breast Cancer Res Treat 2008; 107:1–14.
8. Park SY, Han B-K, Ko ES, et al. Additional lesions seen in magnetic resonance imaging of breast cancer patients: the role of second-look ultrasound and imaging-guided interventions. Ultrasonography 2019; 38:76.
9. Spick C, Szolar DHM, Preidler KW, et al. 3 Tesla breast MR imaging as a problem-solving tool: diagnostic performance and incidental lesions. PLoS One 2018; 13.
10. Meeuwis C, Mann RM, Mus RDM, et al. MRI-guided breast biopsy at 3T using a dedicated large core biopsy set: feasibility and initial results. Eur J Radiol 2011; 79:257–261.
11. Spick C, Baltzer PAT. Diagnostic utility of second-look US for breast lesions identified at MR imaging: systematic review and meta-analysis. Radiology 2014; 273:401–409.
12. Luciani ML, Pediconi F, Telesca M, et al. Incidental enhancing lesions found on preoperative breast MRI: management and role of second-look ultrasound. Radiol Med 2011; 116:886–904.
13. Clauser P, Carbonaro LA, Pancot M, et al. Additional findings at preoperative breast MRI: the value of second-look digital breast tomosynthesis. Eur Radiol 2015; 25:2830–2839.
14. Leung JWT. Utility of second-look ultrasound in the evaluation of MRI-detected breast lesions. Semin Roentgenol 2011; 46:260–274.
15. Koh J, Kim EK, Kim MJ, et al. Additional magnetic resonance imaging-detected suspicious lesions in known patients with breast cancer:

comparison of second-look digital tomosynthesis and ultrasonography. Ultrasound Q 2017; 33:167–173.
16. Mariscotti G, Houssami N, Durando M, et al. Digital breast tomosynthesis (DBT) to characterize MRI-detected additional lesions unidentified at targeted ultrasound in newly diagnosed breast cancer patients. Eur Radiol 2015; 25:2673–2681.
17. Choudhery S, Polley E, Conners AL. Assessment of MRI-detected lesions on screening tomosynthesis in patients with newly diagnosed breast cancer. Clin Imaging 2020; 59:50–55.
18. Cohen JF, Korevaar DA, Altman DG, et al. STARD 2015 guidelines for reporting diagnostic accuracy studies: explanation and elaboration. BMJ Open 2016; 6.
19. Wenkel E, Wunderlich P, Fallenberg EM, et al. Recommendations of the German Radiological Society's breast imaging working group regarding breast MRI. Rofo 2024.
20. Plana MN, Carreira C, Muriel A, et al. Magnetic resonance imaging in the preoperative assessment of patients with primary breast cancer: systematic review of diagnostic accuracy and meta-analysis. Eur Radiol 2012; 22:26–38.
21. Seely JM. Management of breast magnetic resonance imaging-detected lesions. Can Assoc Radiol J 2012; 63:192–206.
22. Kolta M, Clauser P, Kapetas P, et al. Can second-look ultrasound downgrade MRI-detected lesions? a retrospective study. Eur J Radiol 2020; 127.
23. Hellerhoff K, Dietrich H, Schinner R, et al. Assessment of MRI-detected breast lesions: a benign correlate on second-look ultrasound can safely exclude malignancy. Breast Care (Basel) 2021; 16:435–443.
24. Ali A, Phillips J, Ljuboja D, et al. Prospective evaluation of the cost of performing breast imaging examinations using a time-driven activity-based costing method: a single-center study. J Breast Imaging 2023; 5(5):546–554.
25. Chikarmane SA, Jin B, Giess CS. Accuracy of MRI-directed ultrasound and subsequent ultrasound-guided biopsy for suspicious breast MRI findings. Clin Radiol 2020; 75(3):185–193.